NATIONAL AERONAUTICS AND SPACE ADMINISTRATION

Technical Report 32-1286

An Investigation of Spherical Blast Waves and Detonation Waves in a Rocket Combustion Chamber

John M. Bonnell

JET PROPULSION LABORATORY

CALIFORNIA INSTITUTE OF TECHNOLOGY

PASADENA, CALIFORNIA

August 15, 1968

NATIONAL AERONAUTICS AND SPACE ADMINISTRATION

Technical Report 32-1286

An Investigation of Spherical Blast Waves and Detonation Waves in a Rocket Combustion Chamber

John M. Bonnell

Approved by:

D. F. Dipprey, *Manager*
Liquid Propulsion Section

JET PROPULSION LABORATORY
CALIFORNIA INSTITUTE OF TECHNOLOGY
PASADENA, CALIFORNIA

August 15, 1968

TECHNICAL REPORT 32-1286

Prepared Under Contract No. NAS 7-100
National Aeronautics & Space Administration

Contents

Tables

Figures

Contents (contd)

Figures (contd)

Abstract

An investigation was conducted to determine the nature of the shock-like wave produced by an explosion in a liquid propellant rocket combustion chamber. A relatively simple model of the wave behavior was devised. It consisted of a spherical blast wave that developed into a steadily propagating Chapman–Jouguet plane detonation wave. The behavior of the blast wave close to the explosive source was determined by a series of bomb tests conducted in a chamber pressurized with nitrogen. The behavior of a spherical wave in a reacting medium was determined by exploding bombs mounted on the axial centerline of a rocket combustor in a series of rocket motor firings. A comparison of the theoretical and actual times for a wave to travel from its source to the chamber wall indicated that the actual times were appreciably larger. However, the theoretical detonation conditions of the combustion chamber were rather ill-defined and could be adjusted to accommodate the experimental results. The results indicated that the bomb-generated wave, on its first pass to the wall, behaved more like a blast wave than a detonation wave.

An Investigation of Spherical Blast Waves and Detonation Waves in a Rocket Combustion Chamber

I. Introduction

The transition from a stably operating liquid propellant rocket engine to one that exhibits a high-amplitude and destructive, resonant (or oscillatory) mode is sometimes accompanied by the sudden appearance at the wall of a high-amplitude steep-fronted wave that resembles the detonation waves generated in other reacting systems. In some instances, this disturbance is generated spontaneously. In others, it is initiated by a controlled perturbation, such as a bomb. Such waves have been characterized as "detonation-like" waves (Ref. 1). However, in rocket engines, the fact that such waves are generally superimposed upon another combustion process has led to some difficulty in demonstrating that the disturbance is a true detonation wave. In the sense used here, the term "detonation-like" refers to a shock-fronted disturbance that is driven by energy release because of combustion in a very thin zone immediately behind the shock front. This is unlike the more commonly observed type of combustion pressure oscillation, which is not necessarily steep-fronted and is driven by energy release that may occur some distance behind the wave front.

There are several ways by which such waves may be initiated. For example, they may develop spontaneously from the combustion noise, in which case the transition would be very similar to that observed in a gaseous detonation tube. It is equally possible that the initiating source might be the spontaneous, explosive decomposition of a concentrated pocket of propellant. Hydrazine, for example, would exhibit (except for randomness of location) initial characteristics that are approximated by the intentional explosion of a "bomb." Although the early histories of each of these initiating disturbances may be quite different, the resulting detonation-like disturbances are indistinguishable. This investigation is intended to examine the behavior of the blast wave emitted by a bomb exploding in a rocket combustion chamber and the subsequent interaction of the wave with the burning medium. Therefore, the results apply to the explosion-initiated transitions, as suggested above.

The approach employed for studying the problem is to simplify it to the special case of one-dimensional spherical wave propagation, and to tailor the theoretical

analyses and experiments accordingly. There is some relatively recent experimental and theoretical evidence (Refs. 2 and 3) that a spherical detonation wave is initially as either an overdriven or underdriven detonation wave that undergoes a transition to a steadily propagating Chapman–Jouguet detonation wave. Since a bomb explosion is the initiating source in the subject problem, the initial blast wave would be an overdriven wave.

In the present investigation, a relatively simple analysis was conducted in an attempt to describe the wave behavior theoretically. In addition, a series of experiments was conducted to obtain measurements of the behavior of the spherical blast wave emitted by a bomb in both an inert medium and a combustion chamber.

II. Theoretical Analysis

For the analysis, it was assumed that the wave emitted by the explosive source could be described during its transition period by the existing theory of spherical blast waves. It was further assumed that the steadily propagating wave is a Chapman–Jouguet (C–J) detonation wave, also described by existing theory. The hypothesized wave behavior is illustrated in Fig. 1. It is believed that the "patching" together of the blast wave and C–J detonation wave solutions is adequate for a first approximation of the behavior of the wave produced by a bomb in a rocket combustion chamber.

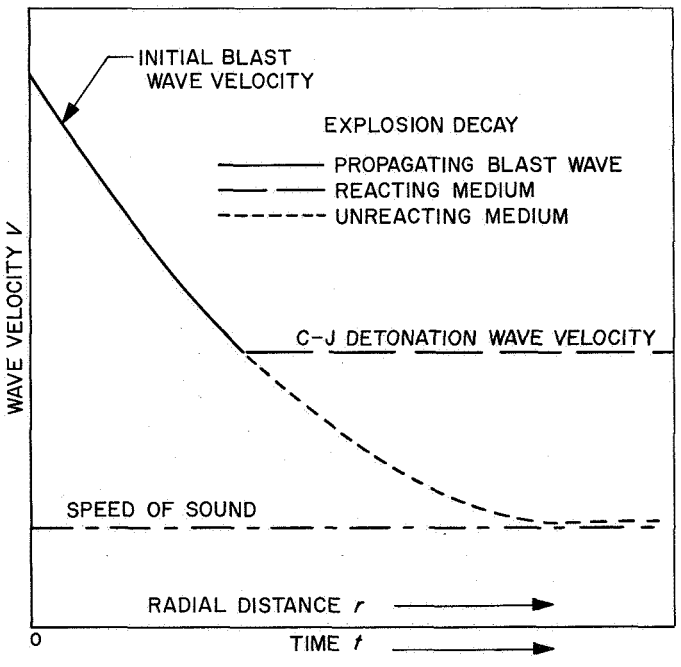

Fig. 1. Hypothesized blast-detonation wave velocities in reacting and nonreacting media

The case of an intense explosion in an inert gaseous medium was treated by Sedov (Ref. 4) utilizing similarity procedures. In this case, the blast wave decayed, as indicated by the dotted line in Fig. 1, asymptotically approaching the speed of sound. The exact solutions for the motion of a blast wave emitted in an explosion are as follows:

for spherical geometry,

$$r^{5/2} = \left(\frac{E}{\rho_1}\right)^{1/2} t$$

$$V^{-5/3} = (0.4)^{-5/3} \left(\frac{E}{\rho_1}\right)^{-1/3} t \qquad (1)$$

for cylindrical geometry,

$$r^2 = \left(\frac{E}{\rho_1}\right)^{1/2} t$$

$$V^{-2} = 4\left(\frac{E}{\rho_1}\right)^{-1/2} t \qquad (2)$$

where

r = radius of the shock

t = time

ρ_1 = density of the undisturbed gas

E = a constant parameter that is some fraction of the total energy liberated in an explosion

V = propagation velocity

The two geometries are given because the initial shape of the blast wave may depend on the shape of the explosive charge. Since the bomb energy release parameter, E, presumed to be some fraction of the total energy of the explosion is difficult to determine analytically, it must be determined experimentally.

The behavior of plane detonation waves in a two-phase reacting medium was investigated by Williams (Ref. 5). He analyzed the Rankine–Hugoniot equations for steady-state detonation in dilute sprays and derived the expressions presented in the Appendix. To determine

the detonation properties of a reacting medium it is necessary to select realistic values of the fraction of total mass flux that is liquid, Z, and the fraction of the total enthalpy of the reacting medium employed to drive the wave, $\hat{H}$. Utilizing an existing steady-state combustion model, which is based upon the vaporization of propellant droplets as they travel toward the nozzle, the mass fraction of the total flowrate, vaporized as a function of chamber length, can be estimated. With this approximation, one may determine a narrow range of Z that seems appropriate for any given axial location.

III. Experimental Program

A two-part experimental program was devised to provide information on spherical wave behavior both in reacting and nonreacting media. The first series of experiments consisted of bomb explosions in a cylindrical chamber pressurized with nitrogen. The object of the experiments was to determine the blast wave behavior close to the bomb and to verify the applicability of the theory by Sedov (Ref. 4).

Although there was an attempt made to utilize records from previous motor firings for this purpose, they were not fruitful for the following reasons: (1) the bomb was mounted at the wall, resulting in three-dimensional wave propagation, which was difficult to analyze; and (2) there is no record of the instant of time at which the bomb exploded. Thus, the estimated values of propagation time are questionable. However, it should be noted that the measured overpressures and the crude estimates of wave propagation velocities that have been made are comparable to those for theoretical Chapman–Jouguet plane detonation waves.

The second part of the experimental program consisted of exploding bombs during test firings of the 18-in. rocket motor. The purpose of the latter experiments was primarily to verify theoretical estimates of the resultant wave behavior.

A. Cold Bomb Test Method and Results

For the cold bomb tests, i.e., explosions in a nonreacting medium, the test setup schematically illustrated in Fig. 2 was employed. The bomb was the same configuration employed in previous motor firings (Ref. 1), and consisted of a Dupont E-83 blasting cap enclosed in a 0.5-in.-OD Micarta shell. The bomb was mounted on the axial centerline of the chamber with the centroid of

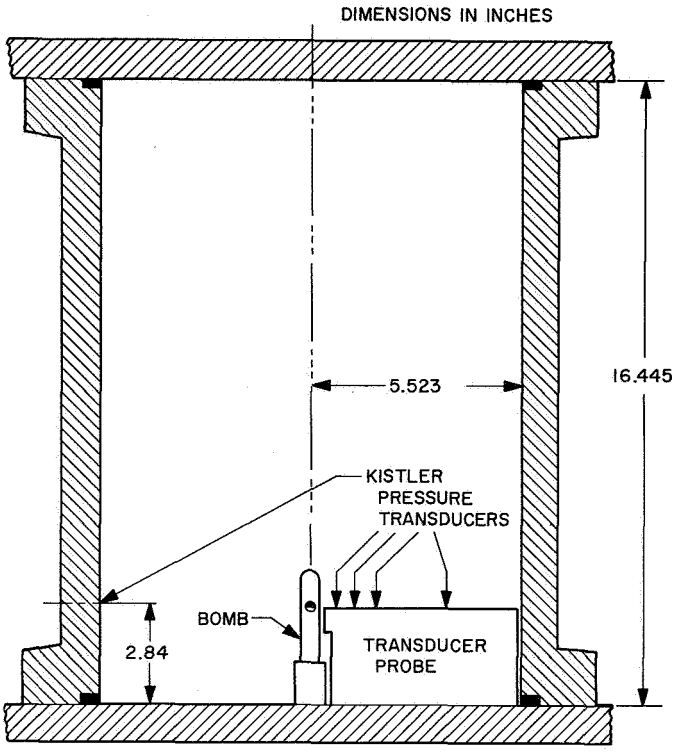

Fig. 2. Setup for cold bomb tests

the explosive charge 2.84 in. from the injector face. That axial location was selected because several Kistler pressure transducers were mounted in that plane in the rocket combustion chambers. In addition, a pressure transducer probe, containing four Kistler pressure transducers, was mounted adjacent to the bomb to measure the blast wave overpressure and propagation velocity at several points close to the explosive source. Additional Kistler pressure transducers were mounted in the wall of the chamber. With the chamber pressurized to 300, 100, and 8 psig, the bombs were exploded.

Five cold bomb tests were conducted at the three chamber pressures, and the data obtained in the tests is summarized in Table 1. From the pressure measurements, it was possible to determine at each transducer location the overpressure and the instant of passage of the blast wave. Thus, the average wave propagation velocity between transducers could be estimated. Utilizing the tables for one-dimensional normal shocks, the shock pressure ratio at each transducer position and a theoretical Mach number were determined. In addition, the bomb parameters E/ρ_1 and E were calculated for each transducer location. Plots of dimensionless time, ta/R, vs dimensionless distance, r/R, were also made to determine the trajectory of the blast wave.

Table 1. Cold bomb test results

Test No.	Pressure, psig	Temperature °R	a ft/s	Pressure transducer position in.	Δt μs	ΔP psi	p_2/p_1	Theoretical M	Mean[a] velocity ft/s	Mean[a] M	E/ρ_1 ft^5/s^2	E lbm/ft^2/s^2	r/R	ta/R
1	300	560(est)	1177	0.681	8.0	3395	11.8	3.20	4480	3.80	0.906×10^4	0.133×10^5	0.123	0.0204
				1.181	—	—	—	—	4170	3.55	—	—	0.214	—
	($\rho_1 = 1.462$ lbm/ft^3)			1.681	28.0	2590	9.26	2.84	4170	3.55	0.682×10^5	0.100×10^6	0.304	0.0714
				3.681	90.0	600	2.83	1.60	2690	2.29	0.340×10^6	0.500×10^6	0.666	0.230
				wall	192.0	710	2.29	1.45	1500	1.275	0.544×10^6	0.800×10^6	1.000	0.502
2	100	560(est)	1177	0.681	6.0	4790	43.2	6.09	5990	5.09	0.161×10^5	0.086×10^5	0.123	0.0153
				1.181	13.0	1455	13.8	3.46	5960	5.06	0.549×10^5	0.292×10^5	0.214	0.0332
	($\rho_1 = 0.53$ lbm/ft^3)			1.681	21.0	1512	14.32	3.52	5210	4.43	0.122×10^6	0.649×10^5	0.304	0.0536
				3.681	67.0	355	4.13	1.92	3630	3.08	0.613×10^6	0.326×10^6	0.666	0.171
				wall	136.0	551	4.64	2.02	2255	1.89	1.12×10^6	0.594×10^6	1.000	0.347
3	301	561	1177	0.681	3.75	5840	11.45	4.00	9580	8.15	0.411×10^5	0.604×10^5	0.123	0.0096
				1.181	11.25	3360	11.7	3.36	5550	4.72	0.734×10^5	0.108×10^6	0.214	0.0288
	($\rho_1 = 1.462$ lbm/ft^3)			1.681	22.0	2810	9.90	2.94	3880	3.30	1.11×10^5	0.163×10^6	0.304	0.0563
				3.681	83.5	450	2.43	1.49	2705	2.30	0.395×10^6	0.580×10^6	0.666	0.214
				wall	174.5	430	1.48	1.19	1785	1.52	0.680×10^6	1.00×10^6	1.000	0.446
4	8	547	1162	0.681	2.22	—	—	—	16,200	13.95	1.18×10^5	0.122×10^5	0.123	0.0056
				1.181	5.93	2260	106.2	9.54	11,200	9.65	2.64×10^5	0.272×10^5	0.214	0.0151
	($\rho_1 = 0.103$ lbm/ft^3)			1.681	14.8	538	26.0	4.78	4680	4.03	2.46×10^5	0.254×10^5	0.304	0.0375
				3.681	46.0	235	11.9	3.21	5340	4.6	1.30×10^6	0.134×10^6	0.666	0.117
				wall	67.8	—	—	—	—	—	4.50×10^6	0.464×10^6	1.000	0.171
5	100	531	1145	0.681	—	—	—	—	8440	7.36	—	—	0.123	—
				1.181	9.2	3070	28.05	4.91	8440	7.36	1.096×10^5	0.611×10^5	0.214	0.0229
				1.681	17.9	1680	15.8	3.69	4790	4.18	1.675×10^5	0.935×10^5	0.304	0.0446
				3.681	61.5	384	4.35	1.97	3820	3.34	0.727×10^6	0.406×10^6	0.666	0.154
				wall	122.0	600	—	—	2540	2.22	1.390×10^6	0.775×10^6	1.000	0.303

[a]Average for next inner interval.

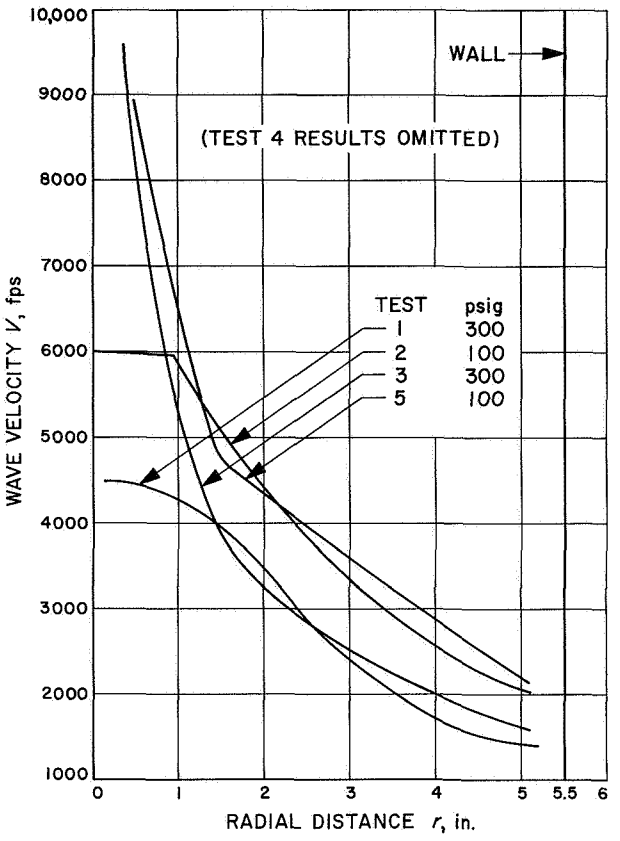

Fig. 3. Average propagation velocity vs radial distance

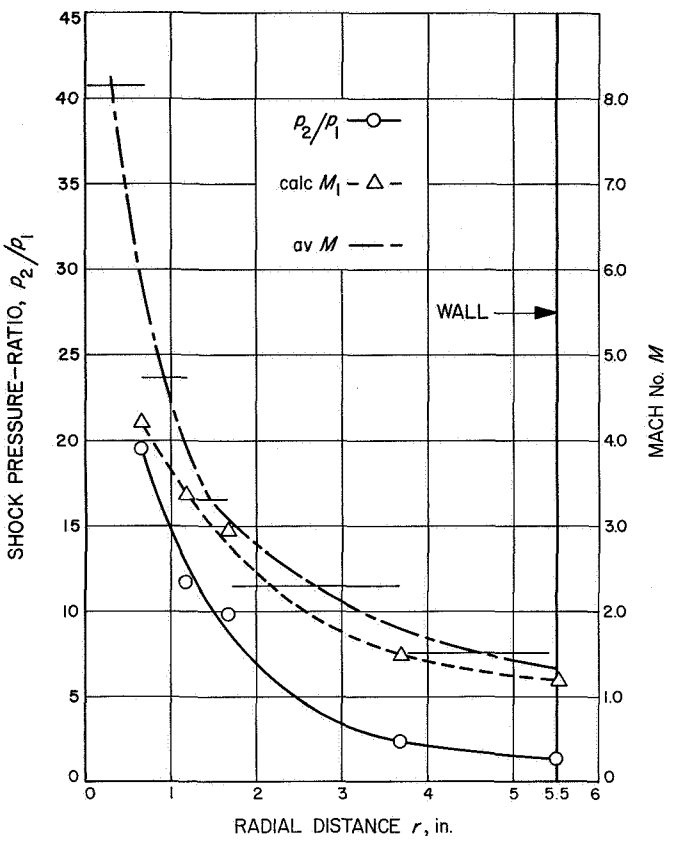

Fig. 4. Shock pressure ratio and average Mach number vs radial distance

Figure 3 presents curves of average propagation velocity vs radial distance for four tests (the results of test No. 4 were omitted). Figure 4 presents plots of the shock pressure ratio, the theoretical Mach number for a plane normal shock based upon the pressure ratio, and the average Mach number calculated from time–distance data, all as functions of radial distance. The results plotted in Fig. 4 reflect test No. 3 only, whereas the comparable results for test Nos. 1, 2, 4, and 5 are presented in Table 1.

The bomb parameters E and E/ρ_1 are plotted as a function of radial distance in Figs. 5 and 6, respectively. Values of E, also determined for cylindrical coordinates for runs 1–3, are presented in Fig. 7. The dimensionless time–distance relationships for the five tests are presented in Fig. 8.

It should be noted that the results of test 4, conducted with a chamber pressure of 8 psig, are questionable. The possibility of erroneous pressure measurements exists and a repeat test was not made to verify the result.

B. Hot Bomb Test Method and Results

For the hot bomb tests, i.e., explosion in a reacting medium, the 18-in.-diam rocket motor was employed to burn N_2O_4 + 50/50 UDMH-N_2H_4 propellants. The bomb was mounted at the axial centerline with the charge centroid 2.84 in. from the injector face, as in the cold tests. Pressure measurements were made utilizing Kistler pressure transducers mounted in the chamber wall and in its plane, and at other locations, both in the chamber wall and injector face.

Four bomb tests were conducted during engine firings. Of the four, the instant of the bomb explosion was recorded on only two tests. The pertinent results from the latter two tests are presented in Table 2. For the other two tests, it was not possible to obtain meaningful wave travel times.

It should be noted that the above results were not obtained under ideal conditions since the 18-in.-diam test motor was spontaneously unstable during all four runs. Prior to the bomb explosion, combustion pressure

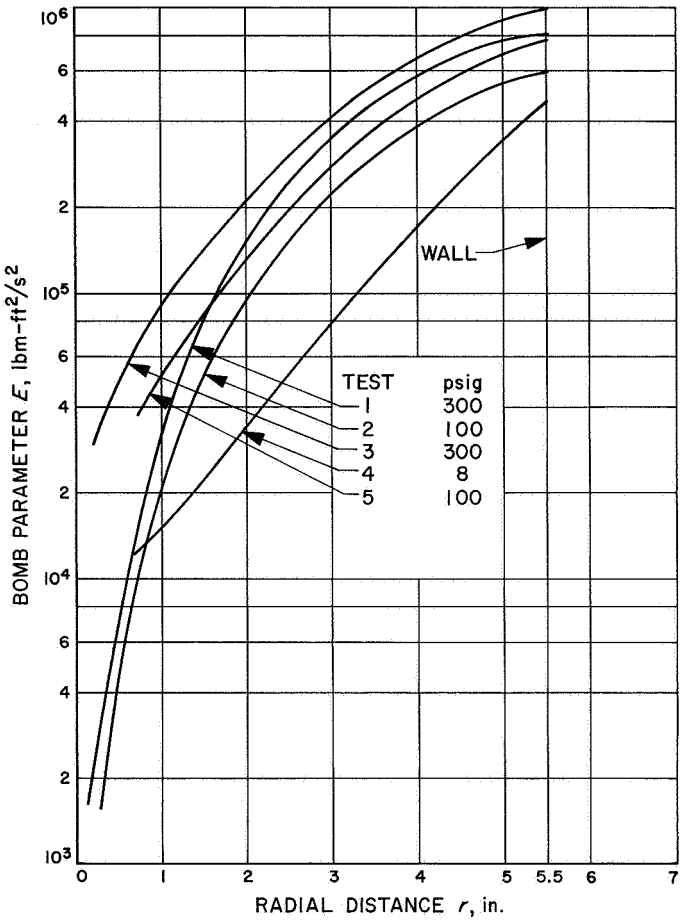

Fig. 5. Parameter *E* plotted as a function of radial distance for spherical coordinates

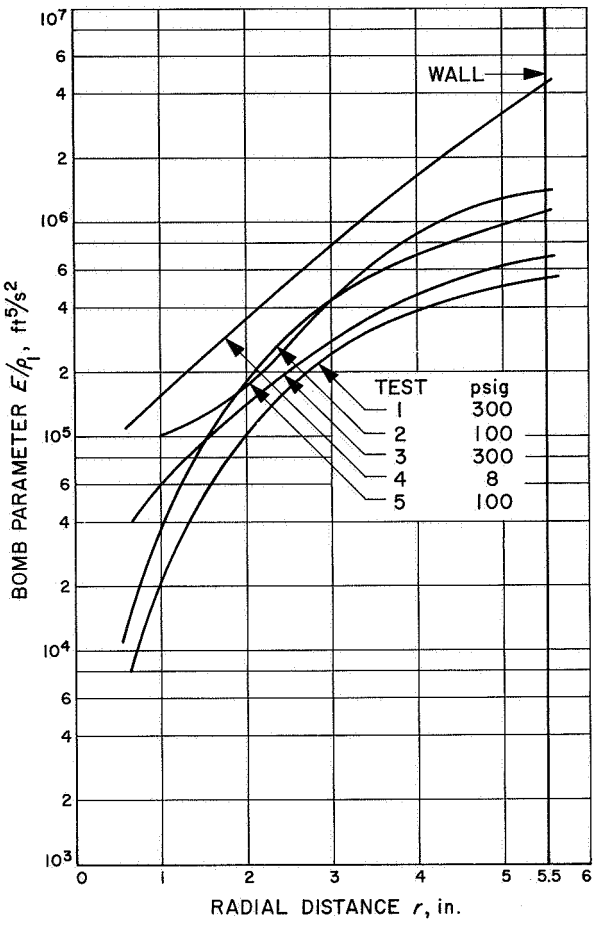

Fig. 6. Parameter E/ρ_1 plotted as a function of radial distance for spherical coordinates

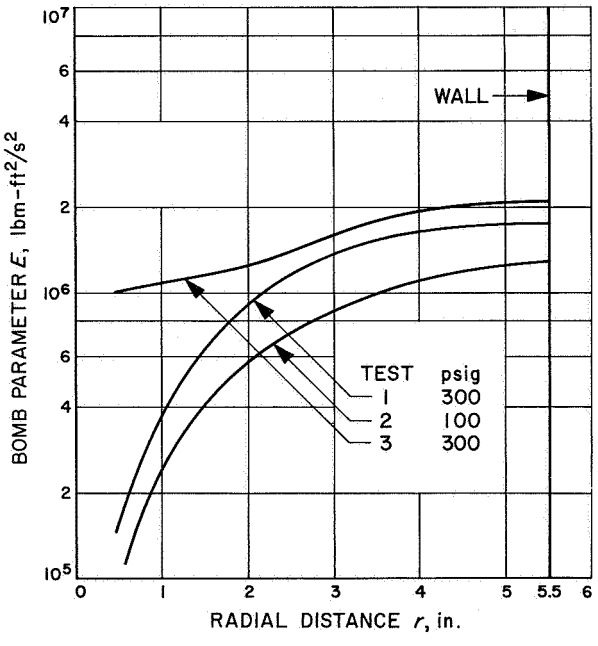

Fig. 7. Parameter *E* vs radial distance, based on cylindrical coordinates

Table 2. Hot bomb test results

Run No.	Parameter[a]	Peak to peak amplitude, psi	Pressure ratio[b]	Wave travel time, μs
B1093[c]	P_c 3130070	118.4	2.32	170.6
	P_c 0880284[d]	205.5	3.28	174.5
	P_c 1630284[d]	119.0	2.33	162.6
	P_c 3130284[d]	162.0	2.80	147.8
	P_c 1890122R	205.5	3.28	71.4
	P_c 2060233R	157.5	2.75	65.8
	P_c 2180356R	197.0	3.19	95.9
	P_c 2330481R	221.0	3.46	112.5
	P_c 2270590R	147.5	2.64	129.1
	P_c 2280801R	68.3	1.76	156.1
B1098[c]	P_c 0880284[d]	136.2	2.51	153.0
	P_c 1630284[d]	82.3	1.92	163.0
	P_c 3130284[d]	135.2	2.50	142.0
	P_c 3131082	—	—	—
	P_c 1890122R	125.5	2.40	66.0
	P_c 2060233R	109.0	2.21	68.4
	P_c 2230481R	69.7	1.78	108.0
	P_c 2270590R	—	—	124.0
	P_c 2280801R	—	—	—

[a]*Transducer location code, e.g.:*
P_c = chamber pressure
189 = circumferential position, deg from reference
0122 = *in.; axial station or radius*
R = radial dimension

[b]Pressure ratio = (pk to pk amplitude + P_c)/P_c

[c]$P_c \simeq 90$ psia; mixture ratio $\simeq 2.0$

[d]Wall-mounted pressure transducers in the 0284 plane

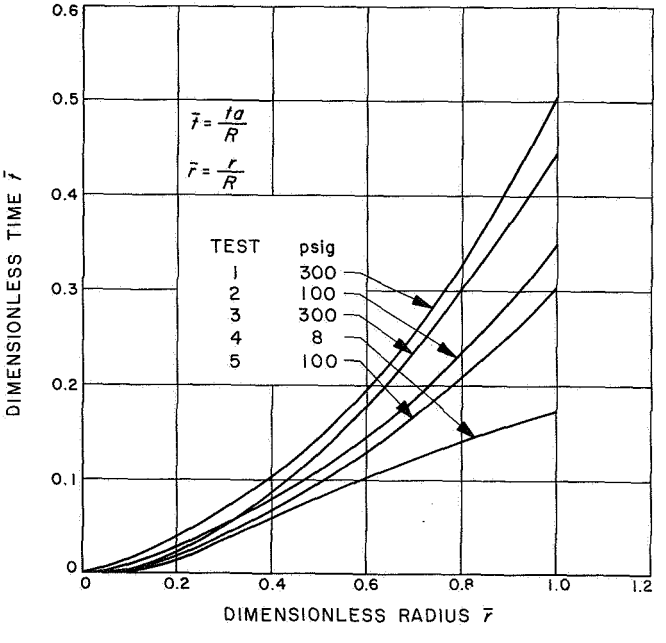

Fig. 8. Dimensionless time–distance relationships ($\bar{t}$ vs $\bar{r}$) for the five tests

oscillations developed during the starting transient. Figure 9 presents some typical pressure records that illustrate the correspondence between the blast wave and the oscillating pressure disturbance.

From Table 2, it is noted that for the transducers mounted in the wall at the 0284-in. plane (P_c 0880284, P_c 1630284, P_c 3130284) the wave travel times varied from 142 to 174.5 μs. It is interesting to note that for the shorter wave travel times, the blast wave (or detonation wave) was in close proximity to the upper crest of the combustion pressure oscillation. A pressure ratio derived from a pressure transducer measurement does not correspond to a theoretical static pressure ratio (p_2/p_1). The pressure transducer measures an impact pressure, which may be amplified by enhanced combustion at the point of impact. Thus, the wave travel time is the preferred parameter for comparing experimental and theoretical results.

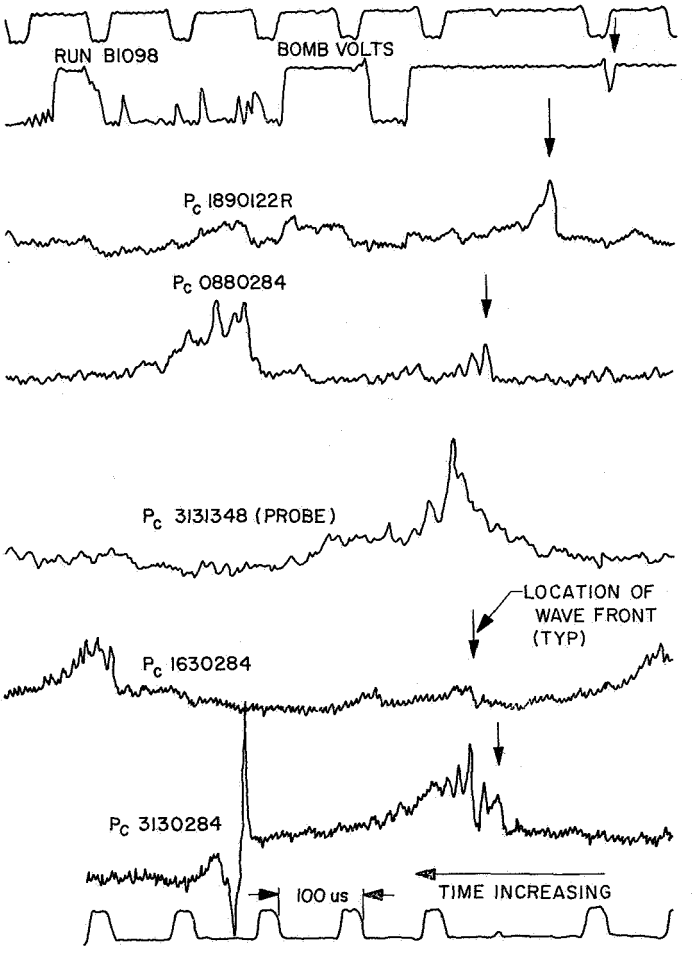

Fig. 9. Transient pressure records

IV. Theory and Experiment Compared

Utilizing the patched blast wave–detonation wave approximation, an estimate may be made of the behavior of a spherical wave initiated at the axial centerline of the 18-in.-diam combustion chamber burning N_2O_4 + 50/50 UDMH-N_2H_4 propellants. The mean combustion pressure and propellant mixture ratio are assumed to be 100 psia and 2.0, respectively. It is further assumed that the combustion gases have a uniform state in the axial plane of interest.

For a specific heat ratio of $k = 1.226$, curves of propagation Mach number and the static pressure ratio for a Chapman–Jouguet detonation wave were generated with a digital computer utilizing the theory attributable to Williams (Ref. 5) (see Appendix). The curves are presented in Figs. 10 and 11 for a wide range of Z and $\hat{H}$. A portion of the results is also presented in Figs. 12 and 13 for relatively narrow ranges of Z and $\hat{H}$ more applicable to this problem.

The static pressure ratio of the hypothesized wave some distance from the source is assumed to be that of a C–J detonation wave. The total wave travel time is given by

$$\Delta t_{\text{total}} = \Delta t_{\text{blast wave}} + \Delta t_{\text{detonation wave}} \qquad (3)$$

The blast wave time is that required for the blast wave to decay to the C–J wave propagation velocity (see Fig. 1) and is determined from Eq. (1) for a spherical wave. The radius at which the C–J detonation wave is assumed to start is determined from Eq. (2). The remaining distance to the chamber wall divided by the propagation velocity of the C–J detonation wave yields $\Delta t_{\text{detonation wave}}$.

A speed of sound of 3935 ft/s, based upon the adiabatic combustion temperature of the above propellants, was employed in the calculations. In addition, calculations were made for smaller values of the speed of sound. In subsequent calculations, the parameter η, defined as $\eta = a/a_o$, is utilized, where a is the local speed of sound and a_o is that for the adiabatic combustion temperature.

Some calculations of the wave travel time as a function of the C–J Mach number and η were performed for

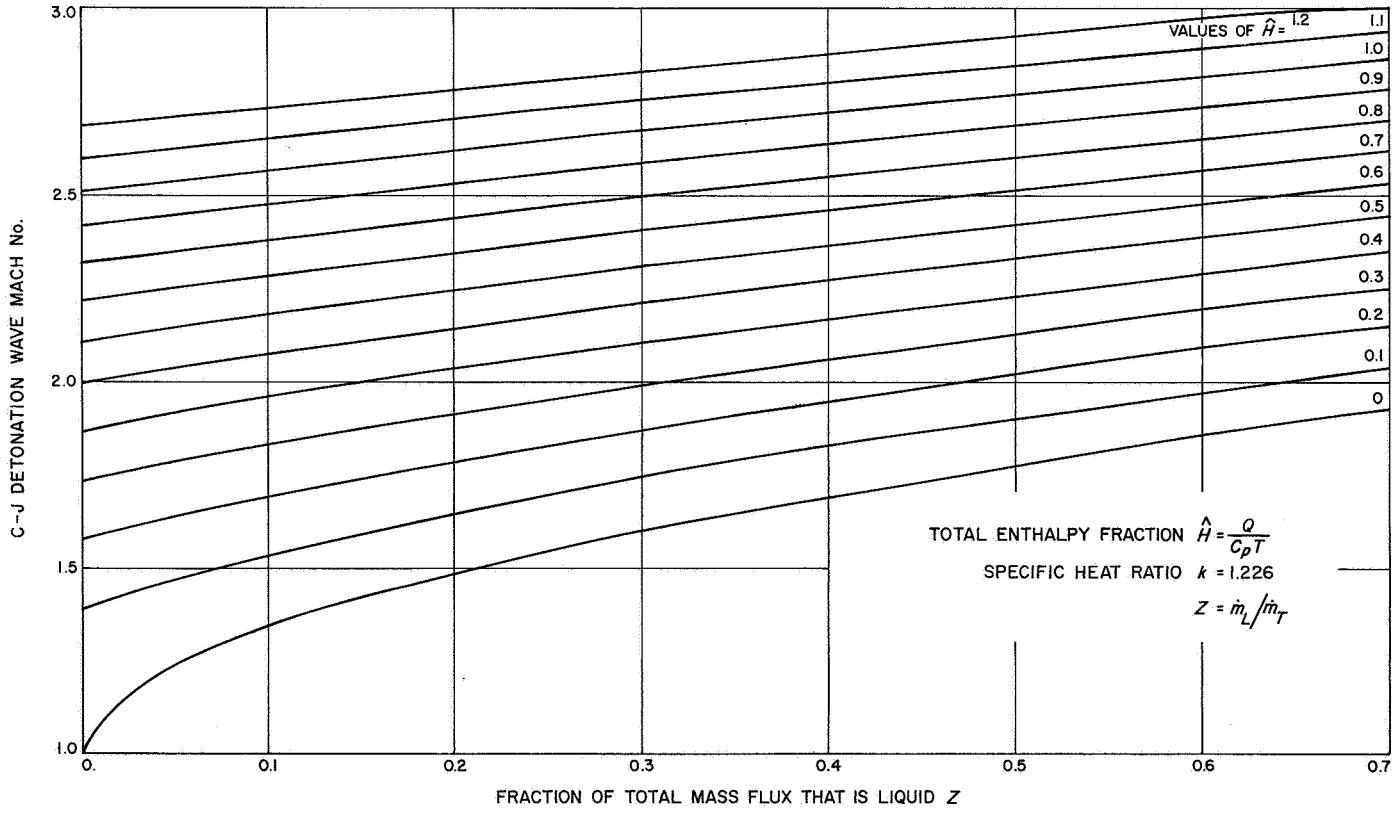

Fig. 10. Chapman–Jouguet detonation wave Mach number vs Z, wide range of Z and $\hat{H}$

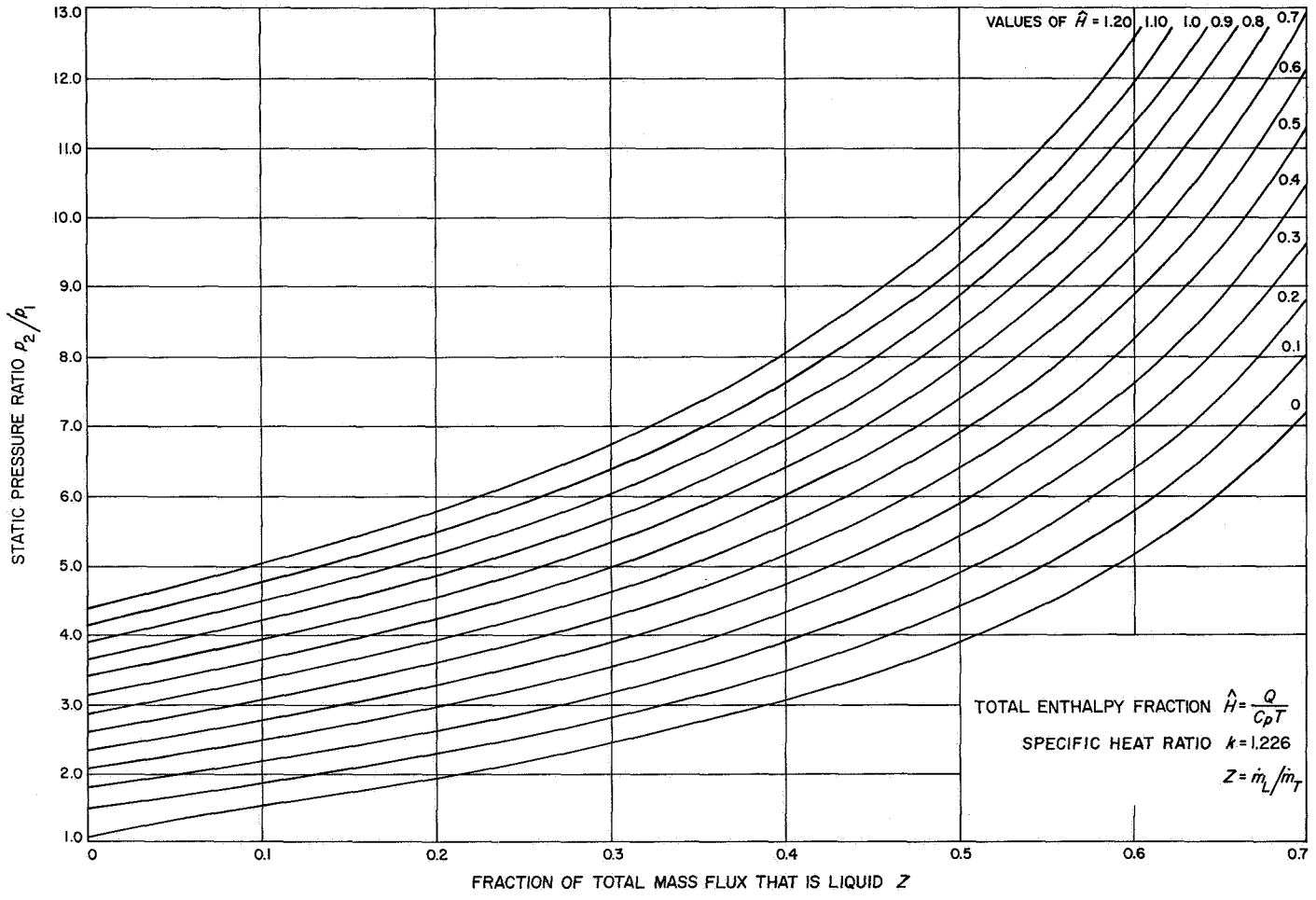

Fig. 11. Chapman-Jouguet detonation wave pressure-ratio vs Z, wide range of Z and $\hat{H}$

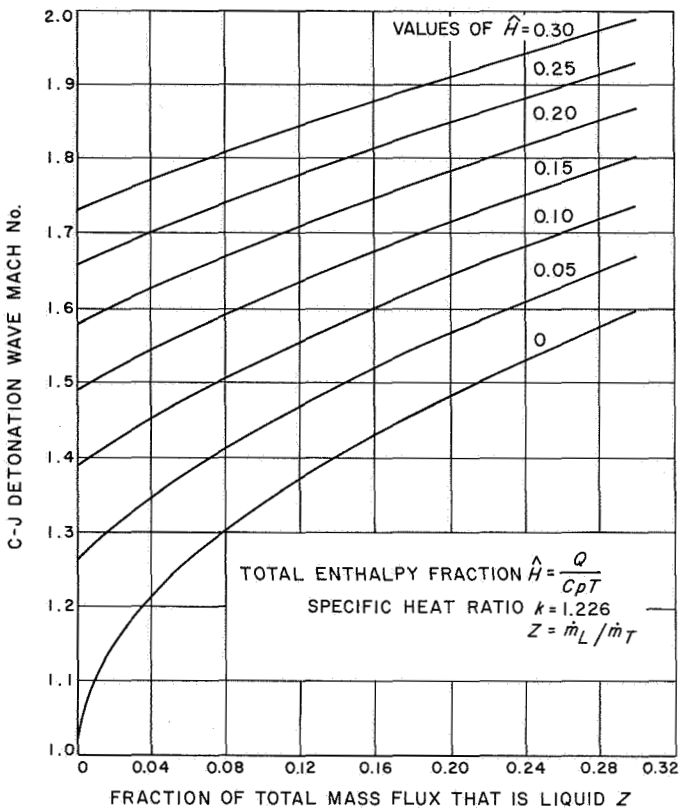

Fig. 12. Chapman–Jouguet detonation Mach number vs Z, narrower ranges of Z and $\hat{H}$

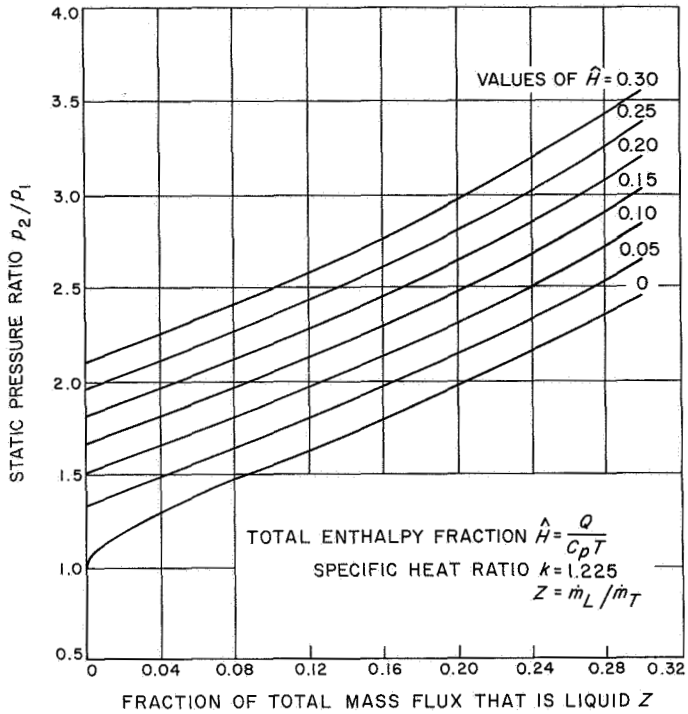

Fig. 13. Chapman-Jouguet detonation wave pressure-ratio vs Z, narrower ranges of Z and $\hat{H}$

the travel-time range of interest. The latter result is presented (see Figs. 14–16) for E values of 10^4, 5×10^4, and 10^5, respectively.

A. Sample Calculation

Referring to Fig. 17, derived from a steady-state combustion model, it is evident that a mass fraction of $Z = 0.30$ is a reasonable value for a distance of 2.84 in. from the injector face. However, it should be noted that the steady-state combustion model is least accurate in the vicinity of the injector. For purposes of this sample calculation, the following range of Z is assumed applicable:

$$0.2 \leq Z \leq 0.3$$

The fraction of the total enthalpy $\hat{H}$, utilized to drive the detonation wave, is assumed to be in the following range:

$$0.0 \leq \hat{H} \leq 0.1$$

From Figs. 10 and 12, one obtains the following range of C–J Mach number (CJM):

$$1.485 \leq \text{CJM} \leq 1.74$$

From Figs. 14 through 16, the following values of wave travel time are obtained for $\eta = 1.0$:

(for $E = 10^4$)	$101.5 \leq \Delta t_{\text{total}} \leq 117.5$ s
(for $E = 5 \times 10^4$)	$96 \leq \Delta t_{\text{total}} \leq 110$ s
(for $E = 10^5$)	$92 \leq \Delta t_{\text{total}} \leq 105.5$ s

The static pressure ratio of the wave immediately before impact with the chamber wall is determined from Figs. 11 and 13, and should be in the following range:

$$1.96 \leq p_2/p_1 \leq 2.84$$

B. Bomb Behavior in an Inert Medium

The results obtained in the few cold bomb tests that have been conducted indicate that the repeatability of the bomb behavior is reasonably good, except very close to the bomb. This is evidenced by comparing the repeat tests in Figs. 3, 5, 6, and 8. The lack of repeatability close to the bomb is probably due to slight differences in the Micarta shells, manufacturer's tolerances in making the blasting caps, and possibly erratic pressure measurements. The strange behavior of the bomb blast in test No. 4 is particularly obvious in the mean velocity calculations (see Table 1). Therefore, it is suspected that

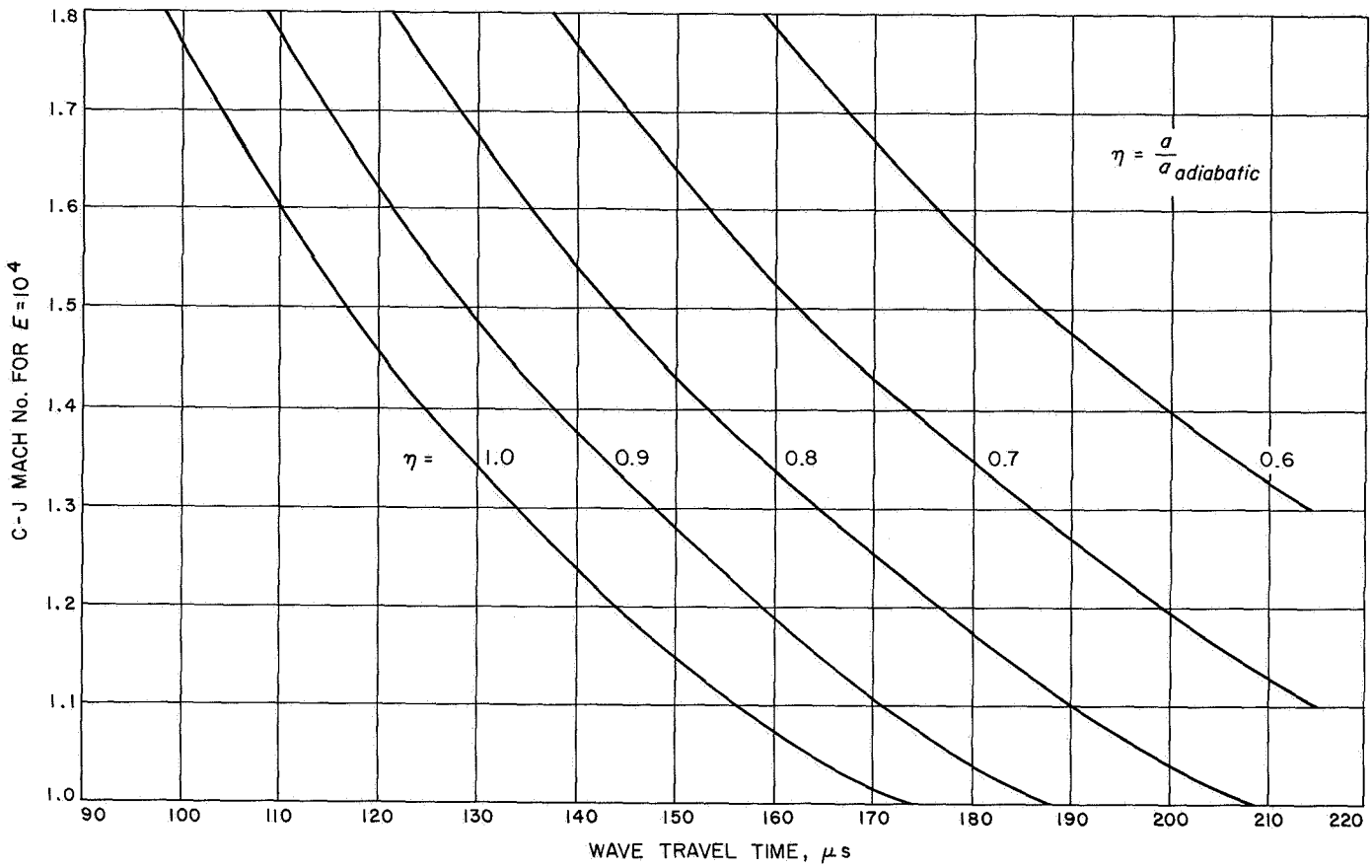

Fig. 14. Wave travel time vs C–J Mach number for $E = 10^4$

the data of test No. 4 may be faulty. It is observed, however, that there is some variation of the bomb behavior with variations in gas pressure and density. Also, test No. 4 results are utilized to a limited extent to indicate the general trend of the blast wave behavior with decreased gas pressure and density.

A comparison of the theoretical plane wave Mach numbers with the average Mach numbers, experimentally determined (see Fig. 4 and Table 1), indicates that there is considerable error in utilizing one-dimensional shock theory for spherical waves very close to the bomb. Since experimentally determined pressure ratios were utilized to determine the theoretical Mach numbers, a part of the apparent error may be due to errors in the pressure measurements.

Figures 5–7 indicate that the blast wave theory of Sedov is not valid in the vicinity of the explosive source, since E and E/ρ_1 are not constants. However, it appears that for the different bomb tests, constant values of E and E/ρ_1 are approached as the radius increases. In this light, the experimentally determined values of E have no physical significance, but they do provide a means of empirically estimating the wave behavior close to the bomb. It should be noted that the predicted wave behavior close to the bomb is approximately the same, utilizing either a spherical or a cylindrical coordinate system (see Figs. 5 and 7).

At this time, it is difficult to select an accurate value of E for blast wave calculations in a combustion chamber. More bomb tests are required in an inert medium at a pressure and density approaching that of the combustion products, and more repeat tests are necessary to increase the confidence level of the results. From the trend of the trial calculations (see Fig. 18) and the trend of E with decreasing density, there is some basis for choosing an E between 10^4 and 10^5 to characterize the type of bomb employed here. Interestingly enough, a difference of one order of magnitude in the selection of E makes a difference of less than 12 μs in the calculation of wave travel time.

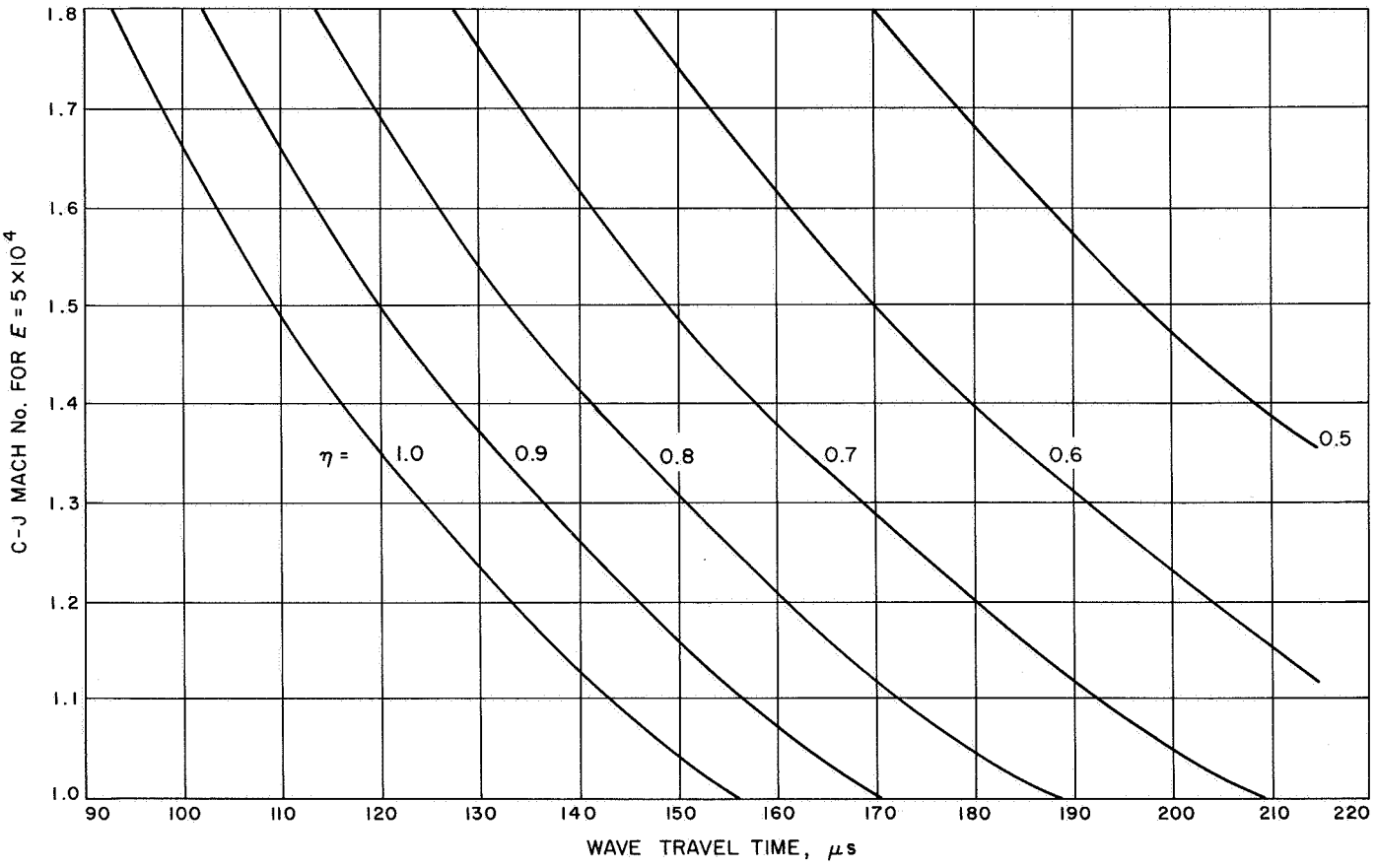

Fig. 15. Wave travel time vs C–J Mach number for $E = 5 \times 10^4$

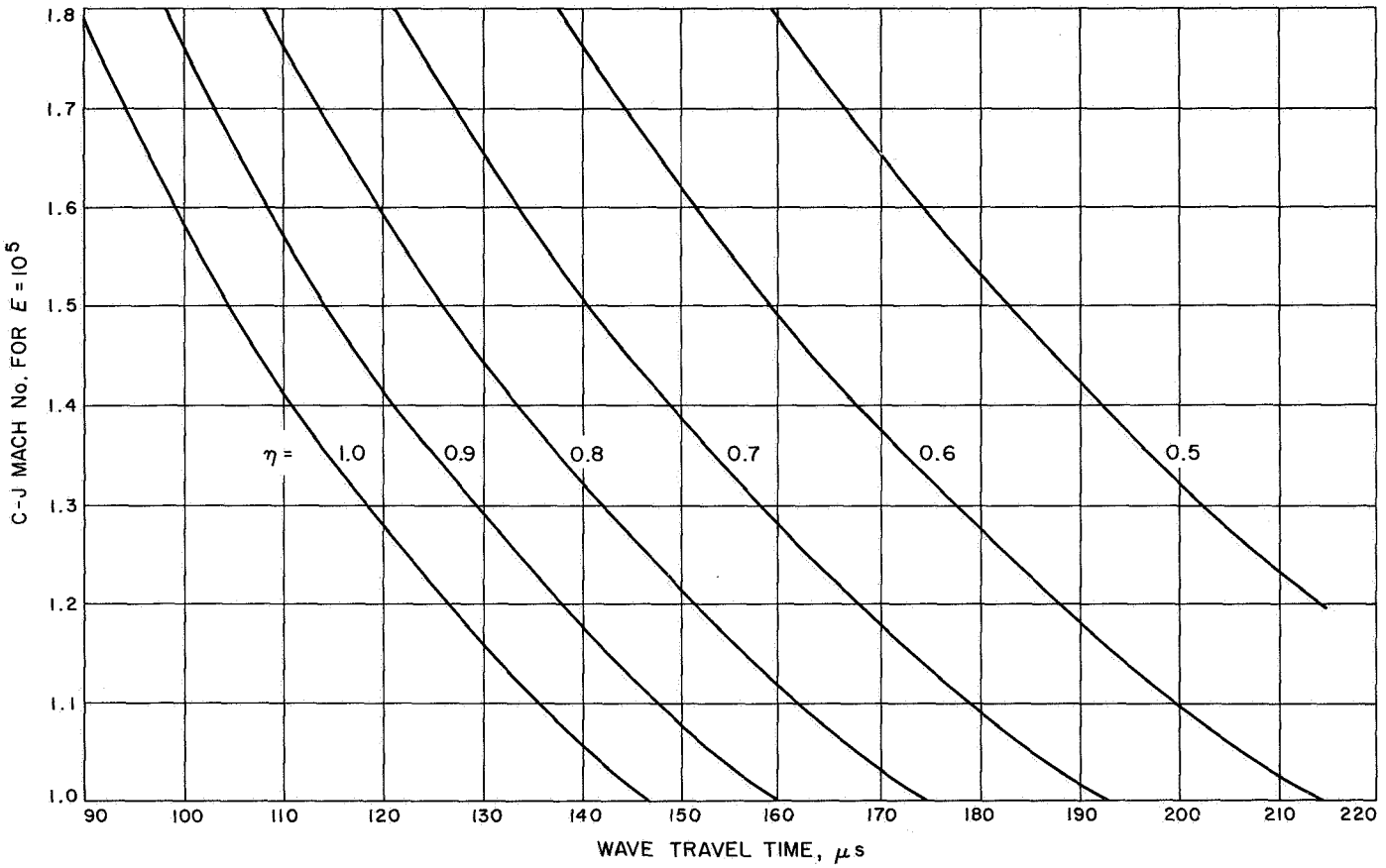

Fig. 16. Wave travel time vs C–J Mach number for $E = 10^5$

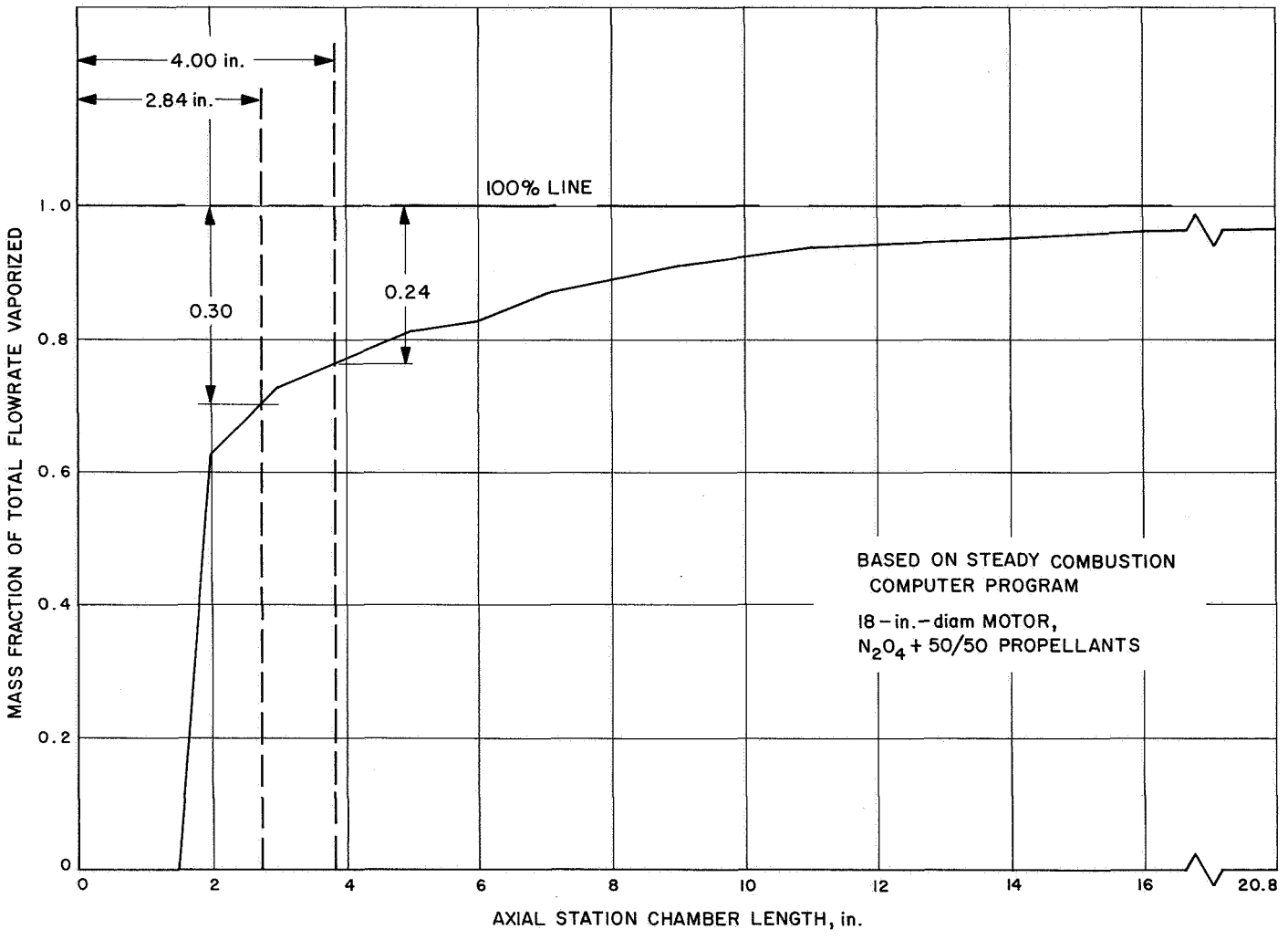

Fig. 17. Axial distribution of vaporized liquid propellant

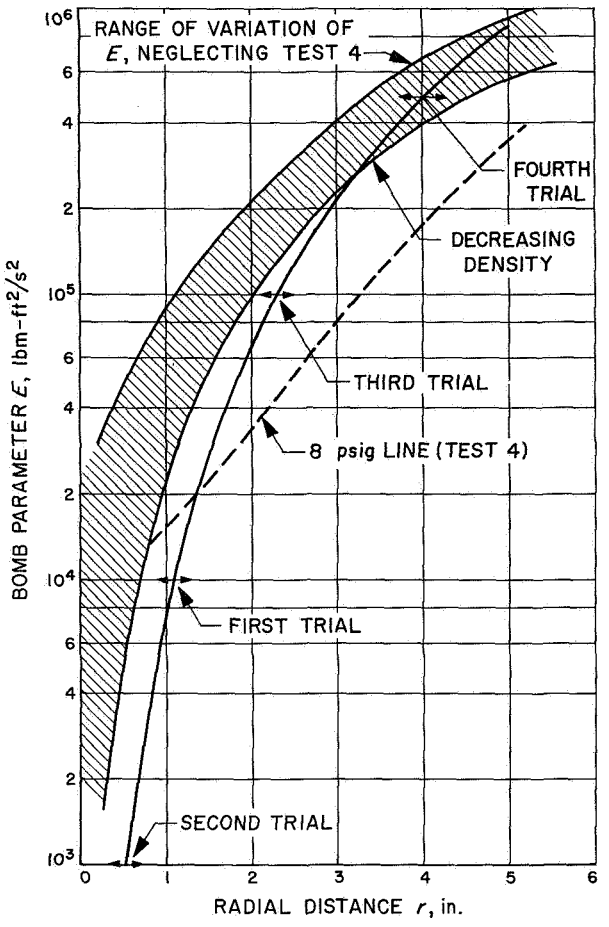

Fig. 18. Selection of parameter E based on four trial calculations

C. Wave Travel Times

The experimental results presented in Table 2 indicate that the wave travel times may be in the vicinity of 142 to 175 μs. The sample calculation, based upon a theoretical steady-state combustion model, and an η of 1.0, resulted in theoretical values in a range of 92 to 118 μs. The agreement between the experimental prediction and the actual result is not good, but this lack of agreement does not necessarily impugn the theoretical wave model employed.

Assuming that the patched wave model is still applicable, the following two factors could account for the low predictions of wave travel time:

(1) The inadequacy of the steady-state combustion model for predicting Z close to the injector face.

(2) The local speed of sound may be less than that based upon the adiabatic combustion temperature ($\eta < 1.0$).

Referring to Figs. 12 and 14 through 16 it is clear that, for small values of Z and $\eta \leq 1.0$, wave travel times within the range of experimentally observed values can easily be obtained. Thus, one may conclude that more information is required concerning the mean liquid droplet mass fraction and the speed of sound in the plane close to the injector, where the measurements are taken. It would also be helpful to have more explicit information on $\hat{H}$ and E, but it is believed that realistic ranges of these parameters were chosen for the sample calculation.

The experimental blast wave measurements obtained during the firing of a rocket combustion chamber were taken during a condition of oscillatory combustion. The nonequilibrium conditions that contributed to the nonuniformity of combustion in each axial plane probably accounts for the difference of approximately 20 and 27 μs in readings between transducers located in the same axial plane. It is difficult to say what wave travel times would be measured during steady-state conditions, although they would probably be close to the observed range of values.

An attempt was made to estimate the local speed of sound in a dispersion of droplets. Existing theory (Ref. 6) indicates that, in an inert medium with droplets having diameters of approximately 10 μm and larger, the speed of sound is unchanged by the presence of the droplets. However, it appears that the subject problem may not be a valid application of a theory designed for aerosols. Undoubtedly, the mean temperature of the gases in the vicinity of the injector is less than the adiabatic combustion temperature.

It is interesting to note that the experimental results indicate that $\hat{H}$ is a very small quantity. If $\hat{H}$ is very close to zero, then the shock wave on its first trip to the wall has the characteristics of a blast wave rather than a detonation wave. After impacting with the chamber wall, the wave could very likely develop into a detonation wave in its subsequent travel throughout the chamber.

V. Concluding Remarks

This work represents a starting point for understanding the behavior of spherical waves in a combustion chamber. Based on the experimental and analytical findings to date, conclusions may be made with respect to inert and combustion chamber environments.

A. Inert Environments

(1) There is considerable difference in bomb behavior in an inert medium as the ambient pressure and density vary.

(2) There is a reasonable degree of repeatability of the behavior of the bomb blast waves investigated in an inert medium, except in the immediate vicinity of the bomb.

(3) The explosive blast wave theory, attributed to Sedov, is not valid close to the explosive source.

(4) Inaccurate results are obtained when one-dimensional shock wave theory is applied to spherical shocks in the vicinity of the bomb.

B. Combustion Chamber Environments

(1) There is insufficient knowledge of the state of the burning liquid-gas medium close to the injector to accurately determine the local detonation properties and the speed of sound.

(2) The total enthalpy fraction ($\hat{H}$) utilized to drive a blast wave (at least on its first pass to the wall) is very small. Thus, the wave may more accurately be described as a blast wave rather than a detonation wave.

This investigation has shown that the behavior of a blast wave on its initial pass to the chamber wall is governed to a very large extent by the local detonation properties of the burning medium. An interesting corollary, which may be derived from this study, is that the blast wave measurements be employed to determine the detonation properties of the gases. This requires an acceptance of the blast wave–C–J detonation wave model. By measuring the wave travel time, and by assuming E and η, one may derive the CJM. The latter parameter is a detonation property of the burning medium that is a function of Z and $\hat{H}$. A first estimate of Z is achieved immediately by letting $E = 10^4$, $\eta = 1.0$, and $\hat{H} = 0$.

Appendix

Chapman-Jouguet Detonation Properties in a Dilute Spray

Williams (Ref. 5) investigated the characteristics of plane detonation waves in a mixture of reacting gases and liquid droplets. From his theoretical analysis of the Rankine–Hugoniot equations, the following expressions for Chapman–Jouguet waves were derived:

$$\frac{\rho_1}{\rho_2} = \frac{u_2}{u_1} = H + 1 - \left[H^2 + \left(\frac{2}{k+1}\right) H\right]^{1/2}$$

$$\frac{p_2}{p_1} = k\left\{H + \frac{1}{k} + \left[H^2 + \left(\frac{2}{k+1}\right) H\right]^{1/2}\right\}$$

$$\frac{T_{g2}}{T_{g1}} = (1 - Z)(k - 1)\left\{\left(\frac{k^2+1}{k^2-1}\right) H + \frac{1}{k-1} + \left[H^2 + \left(\frac{2}{k+1}\right) H\right]^{1/2}\right\}$$

$$M^2 = (1 - Z)(k + 1)\left\{H + \frac{1}{k+1} + \left[H^2 + \left(\frac{2}{k+1}\right) H\right]^{1/2}\right\}$$

where

ρ_2 = density of gas behind the wave

u = gas velocity

k = specific heat ratio

p = static pressure

T_g = gas temperature

Z = fraction of the total mass flux that is liquid

$H = (\hat{H} + Z)/(1 - Z)$

$\hat{H} = Q/C_pT_{g1}$

C_p = specific heat

Q = total heat release per unit mass

M = Mach number of the detonation wave, relative to the undisturbed medium and the subscripts

1 = upstream properties

2 = downstream properties

g = gas property

References

1. Clayton, R. M., and Rogero, R. S., *Experimental Measurements on a Rotating Detonation-Like Wave Observed During Liquid Rocket Resonant Combustion,* Technical Report 32-788. Jet Propulsion Laboratory, Pasadena, Calif., Aug. 15, 1965.

2. Lee, J. H., Lee, B. H. K., and Shanfield, I., "Two-Dimensional Unconfined Gaseous Detonation Waves," *Tenth Symposium (International) on Combustion,* pp. 805–815, The Combustion Institute, Pittsburgh, 1965.

3. Manson, N., and Ferrie, F., "Contribution to the Study of Spherical Detonation Waves," *Fourth Symposium (International) on Combustion,* pp. 486–494, Williams and Wilkins Co., Baltimore, 1953.

4. Sedov, L. I., *Similarity and Dimensional Methods in Mechanics,* pp. 210–232, Academic Press, New York, 1959.

5. Williams, F. A., "Detonations in Dilute Sprays," *Detonation and Two-Phase Flow, Progress in Astronautics and Rocketry,* Volume 6, pp. 99–114. Edited by S. S. Penner and F. A. Williams, Academic Press, New York, 1962.

6. Temkin, S., and Dobbins, R. A., "Attenuation and Dispersion of Sound by Particulate-Relaxation Processes," *J. Acoust. Soc. Am.,* Vol. 40, No. 2, pp. 317–324, 1966.

Bibliography

A. Spherical and Cylindrical Detonation Waves and Blast Waves

1. Boyer, D. W., *Spherical Explosions and Implosions.* UTIA Report 58 (AD-237850), Institute of Aerophysics, University of Toronto, Nov. 1959.

2. Brode, H. L., "Numerical Solutions of Spherical Blast Waves," *J. Appl. Phys.,* Vol. 26, No. 6, pp. 766–775, June 1955.

3. Courant, R., and Friedricks, I. O., *Supersonic Flow and Shock Waves,* pp. 424–433, Interscience Publishers, Inc., New York, 1948.

4. Fay, J. A., "Two-Dimensional Gaseous Detonations: Velocity Deficit," *Phys. Fluids,* Vol. 2, No. 3, pp. 283–288, May–June 1959.

5. Feldovich, Ia. B., Kogarko, S. M., and Simonov, N. N., "An Experimental Investigation of Spherical Detonation of Gases," *Soviet Physics, Technical Physics,* Vol. 1, No. 8, pp. 1689–1713, 1957.

6. Fox, P., and Ralston, A., "On the Numerical Solution of the Equations for Spherical Waves of Finite Amplitude, I," *J. Math. Phys.,* Vol. 36, pp. 313–328, 1957.

Bibliography (contd)

7. Friedricks, I. O., and Keller, J. B., "Geometrical Acoustics II, Diffraction, Reflection, and Refraction of a Weak Spherical or Cylindrical Shock at a Plane Interface," *J. Appl. Phys.*, Vol. 26, No. 8, pp. 961–966, Aug. 1955.

8. Friewald, H., and Koch, H. W., "Spherical Detonations of Acetylene-Oxygen-Nitrogen Mixtures as a Function of Nature and Strength of Initiation," *Ninth Symposium (International) on Combustion*, pp. 275–281, Academic Press, New York, 1963.

9. Glass, I. I., and Heuckroth, R., *An Experimental Investigation of the Head-On Collision of Spherical Shock Waves*, Institute of Aerophysics, University of Toronto, UTIZ Report 59 (AD-240354), May 1960.

10. Latter, R., "Similarity Solution for a Spherical Shock Wave," *J. Appl. Phys.*, Vol. 26, No. 8, pp. 954–960, Aug. 1955.

11. Lee, J. H., *The Propagation of Shocks and Blast Waves in a Detonating Gas*, Report 65-1, Gasdynamics Research Laboratory, McGill University, Toronto, Mar. 1965.

12. Lewis, C. H., *The Blast-Hypersonic Flow Analogy Based Upon Oshima's Quasi Similarity Model*, ARO, Report AEDC-TN-61-158 (AD-268639). Dec. 1961.

13. Lin, Shao-Chi, "Cylindrical Shock Waves Produced by Instantaneous Energy Release," *J. Appl. Phys.*, Vol. 25, No. 1, pp. 54–57, Jan. 1954.

14. Lyubimov, G. A., "The Effect of Viscosity and Heat Conduction on the Flow of a Gas Behind a Severely Curved Shock Wave," *Moscow U. Vestnik, Seriya Matematik, Mekhaniki, Astronomii, Fiziki Khimii (USSR)* [v. 13] no. 5, pp. 33–35, 1958. Translation available as FTD-TT-61-266/1 + 2 (AD-270763), Jan. 25, 1962.

15. Plesset, M. S., "On the Stability of Fluid Flows with Spherical Symmetry," *J. Appl. Phys.*, Vol. 25, No. 1, pp. 96–98, Jan. 1954.

16. Roberts, L., "On the Numerical Solution of the Equations for Spherical Waves of Finite Amplitude, II," *J. Math. Phys.*, Vol. 36, pp. 329–337, 1957.

17. Schardin, H., "Measurement of Spherical Shock Waves," *Commun. Pure Appl. Math.*, Vol. VII, pp. 223–243, 1954.

18. Shin, Y., *Attenuation of Repeated Spherical Shock Waves*, UCLA Technical Report 22 (AD-413346), July 1963.

19. Taylor, J. L., "An Exact Solution of the Spherical Blast Wave Problem," *Phil. Mag.*, No. 46, pp. 317–320, Mar. 1955.

20. Taylor, G. I., "The Dynamics of the Combustion Products Behind Plane and Spherical Detonation Fronts in Explosives," *Proc. Roy. Soc. London, Ser. A*, Vol. 200, pp. 235–247, Jan. 1950.

21. Zeldovich, Ia. B., and Kompaneets, A. S., *Theory of Detonation*, pp. 56, 279, Academic Press, New York, 1960.

Bibliography (contd)

B. Detonation Wave Property Calculations

1. Bollinger, L. E., and Edse, R., "Thermodynamic Calculations of Hydrogen-Oxygen Detonation Parameters for Various Initial Pressures," *ARS J.*, pp. 251–256, Feb. 1961.
2. Edse, R., *Calculations of Detonation Velocities in Gases,* WADC Technical Report 54-416, Mar. 1956.
3. Gillespie, R. D., and Warga, J., *A Program for Computing Thermochemical Equilibrium Behind a Moving Shock Wave,* AVCO Corporation Technical Memorandum RAD-TM-63-65 (AD-417641), Sept. 23, 1963.
4. Zeleznik, F. J., and Gordon, S., "Calculation of Detonation Properties and Effect of Independent Parameters on Gaseous Detonations," *ARS J.*, pp. 606–615, Apr. 1962.
5. Zeleznik, F. J., and Gordon, S., *A General IBM 704 or 7090 Computer Program for Computation of Chemical Equilibrium Compositions, Rocket Performance, and Chapman–Jouguet Detonations,* NASA TN D-1454, National Aeronautics and Space Administration, Washington, Oct. 1962.

C. Measurement Techniques

1. Combs, L. P., et al., *Combustion Stability Rating Techniques,* Third Quarterly Progress Report, Rocketdyne Report R 6355-3, Apr. 1966.
2. Dunn, M. G., and Blum, R. J., *Continuous Measurement of Shock Velocity Using a Microwave Technique,* NASA CR-490, National Aeronautics and Space Administration, Washington, May 1966.
3. Ruetenik, J. R., and Lewis, S. D., *Pressure Probe and System for Measuring Large Blast Waves,* Technical Report AFFDL-TDR-65-35, M.I.T. (AD-467828), June 1965.
4. Schardin, H., "Measurement of Spherical Shock Waves," *Commun. Pure Appl. Math.*, Vol. VII, pp. 223–243, 1954.

D. Numerical Mathematical Techniques

1. Burstein, S. Z., *Finite Difference Calculations for Hydrodynamic Flows Containing Discontinuities,* AEC Research and Development Report NYO-1480-33, New York University, Sept. 1964.
2. Burstein, S. Z., "Numerical Methods in Multidimensional Shocked Flow," *AIAA J.*, Vol. 2, No. 12, pp. 2111–2117, Dec. 1964.
3. Fox, L., *Numerical Solution of Ordinary and Partial Differential Equations,* pp. 325–365, Pergamon Press, New York, 1962.
4. Houghton, D., Kasahara, A., and Washington, W., "Long-Term Integration of the Baratropic Equations by the Lax–Wendroff Method," *Monthly Weather Review,* Vol. 94, No. 3, pp. 141–150, Mar. 1966.
5. Lax, P. D., "Hyperbolic Systems of Conservation Laws II," *Commun. Pure Appl. Math.*, Vol. 10, pp. 537–566, 1957.

Bibliography (contd)

6. Lax, P. D., and Wendroff, B., "Systems of Conservation Laws," *Commun. Pure Appl. Math.*, Vol. 13, pp. 217–237, 1960.

7. Lax, P. D., "Weak Solutions of Nonlinear Hyperbolic Equations and Their Numerical Computation," *Commun. Pure Appl. Math.*, Vol. 7, pp. 159–193, 1954.

8. Lax, P. D., and Wendroff, B., "Difference Schemes for Hyperbolic Equations With High Order of Accuracy," *Commun. Pure Appl. Math.*, Vol. 16, pp. 381–398, 1964.

9. Richardson, D. J., "The Solution of Two-Dimensional Hydrodynamic Equations by the Method of Characteristics," *Methods in Computational Physics*, Vol. 3, pp. 295–318. Edited by B. Alder, S. Fernbach, and M. Rotenberg, Academic Press, New York, 1964.

10. Sauerwein, H., *The Calculation of Two- and Three-Dimensional Inviscid Unsteady Flows by the Method of Characteristics*, M.I.T. (AD-605324), June 1964.

11. Von Neumann, J., and Richtmyer, R. D., "A Method for the Numerical Calculation of Hydrodynamic Shocks," *J. Appl. Phys.*, Vol. 21, pp. 232–237, Mar. 1950.